*The Aeronautical Journal* (2023), **127**, pp. 1698–1716
doi:10.1017/aer.2023.31

**REGULAR PAPER**

# Quantifying the impact of heat in support seal configuration for aero engines

P. Sun[1] and C. Liu[2]

[1]National Key Laboratory of Strength and Structural Integrity, AVIC Aircraft Strength Research Institute, Xi'an, China and [2]School of Power and Energy, Northwestern Polytechnical University, Xi'an, China
**Corresponding author:** P. Sun; Email: sunpeng2016@hotmail.com

**Received:** 5 May 2022; **Revised:** 23 January 2023; **Accepted:** 23 March 2023

**Keywords:** Aero engine; Seal; Clearance; Power loss

## Abstract

Leakage, deformations, power loss, heat generation in the support seal system and other issues are typical when support seals are developed. The design of the support seal system has progressively evolved over recent decades as part of an ongoing effort to provide effective cooling for the aero engine secondary air system. In particular, oil heat management in the oil chamber has strict requirements, which limit the heat generation of the support seal system. The potential of supporting seal research with an oil system is investigated in this work. The combination of the CFD/FEA method and quantifying the heat generation entering the oil chamber allows for improvements not just to the individual buffer air seal unit, but the oil seal together. The analysis relies on the combination of quantifying heat generation entering the oil chamber to provide a mutual influence of neighbouring labyrinth seals. The mutual influence requires further analysis, considering the thermal deformation of the rotor/stator to provide further accurate geometry parameters in preliminary seal designs. The experimental test was conducted to verify the preliminary CFD-FEA loosely coupled analysis result, which reveals that in a turbine support seal system, the radius of the buffer air seal has a significant influence on the leakage flow rate and power loss of the oil seal, which should take into account the integral influence of the pressure difference of the oil seal caused by the radius change of the buffer air seal and the running clearance of the oil seal.

## Nomenclature

| | |
|---|---|
| $Q$ | heat generation |
| $\alpha$ | heat transfer coefficient |
| $F_s$ | surface area of the smooth wall |
| $F_p$ | surface area of the fin |
| $\lambda_{wall}$ | wall thermal conductivity |
| $\Pi_p$ | fin circumference |
| $h_p$ | height of fin |
| $\delta_{wall}$ | wall thickness |
| $C$ | total drag coefficient |
| $\beta$ | coefficient taking into account the effect of radial clearance on power loss |
| $C_p$ | specific heat capacity of air |
| $l$ | diameter of the rolling elements |
| $u$ | circumferential speed of the bearing cage |
| $Re$ | Reynold number |
| $Pr$ | Prandtl number |
| $k$ | thermal conductivity of the oil |
| $Eu$ | Euler number |
| $F_m$ | average load on the bearing |

| | |
|---|---|
| $F_r$ | radial load on the bearing |
| $F_c$ | centrifugal load of the rolling elements in the bearing |
| $d_m$ | diameter of the centre of gravity of the bearing |
| $h_{bearing}$ | value of radial clearance in the bearing |
| $\eta$ | efficiency of gearing system |
| $N$ | transmitted power |
| $\varepsilon_s$ | contact ratio |
| $f$ | coefficient of friction |
| $\beta_g$ | angle of inclination of teeth to the axis of rotation of the starting cylinder |
| $Z_K$ | the number of teeth in driver gear |
| $Z_k$ | the number of teeth in driven gear |

## 1.0 Introduction

Aero engine seals, such as flow path seals and support seals, are unique, one-of-a-kind designs with no natural counterparts. The design of an aero engine support seal is closely tied to the creation of a novel technical approach. The process of developing seals should take into account diverse operating conditions of aviation engines, resulting in high air seal costs and high dependability requirements. The creation of an aero engine support seal is predicated on the resolution of a complicated interrelated challenge. It is necessary to examine both the gas dynamic and thermal expansion of the fluid and solid zones simultaneously. The aero engine support seal can withstand temperatures of up to 1,000°C, pressure variations of up to 1MPa, and circumferential speeds of up to 300m/s. Carbon seal and labyrinth seal are the most used aero engine support seals.

The advancement of aero engine design is matched by the advancement of the secondary air system cooling scheme, which was suggested as a cooling scheme with a buffer chamber (Fig. 1). The intermediate (III) and oil (I) chambers are separated in this design by two chambers: the pre-oil chamber (II) and the buffer chamber. The pre-oil chamber's cooling air goes into both the buffer chamber and the oil chamber. Between the pre-oil chamber and the intermediate chamber lies the buffer chamber. This configuration is more efficient in lowering the temperature of the bearing walls, although leakage into the oil chamber remains substantial. Many studies have been conducted to describe the leakage characteristics caused by labyrinth seals. Ludwig and Johnson [1] examined minimising leakages by reducing seal clearances, which results in rubbing contact, and then determining the ultimate seal clearances based on the seal's temperature response and wear. Povinelli et al. [2] proposed that certain bearing and seal criteria for support seal systems be increased in the development of aero engine thrust and fuel consumption. Proctor et al. [3] described engine manufacturers' worries regarding heat generation and power loss caused by labyrinth seals. Chupp et al. [4] investigated that clearance control is critical for aero engine designers since it is essential to satisfy today's stringent thrust output and efficiency. Excessive clearances reduce engine efficiency, thus cause flow instabilities. Inadequate clearances restrict coolant flows and induce contact between the rotor and stator. Chew et al. [5] illustrated how CFD is often utilised in industry for air system assessment, and how the addition of three-dimensional geometrical properties, as well as the computation of unstable flows, is becoming increasingly common. Aslan-zada et al. [6] investigated the leakage characteristics of brush seals and labyrinth seals. The necessity of proper clearance management and the resulting reduction in parasitic flows is emphasised. Through testing and numerical simulation, von Plehwe et al. [7] described oil leakage across a conventional labyrinth seal used in aircraft engine bearing chambers. Flouros et al. [8] studied the flow through windback seals and their capacity to repel oil that may migrate from a nearby bearing chamber, especially when the pressure difference over the seal is modest. Li et al. [9] discovered an appropriate seal geometry for achieving the highest oil sealing performance. Furthermore, increasing sealing clearance and pitch is detrimental to oil sealing. Li et al. [10] also evaluated the oil sealing performance of two distinct floating ring seals for aero engines in cold and hot states. Ilieva et al. [11] investigated the design and numerical analysis of a labyrinth seal geometry, which contributes to a large reduction in leakage mass flow rates, potentially enhancing the efficiency of turbine as part of an aero engine.

https://doi.org/10.1017/aer.2023.31 Published online by Cambridge University Press

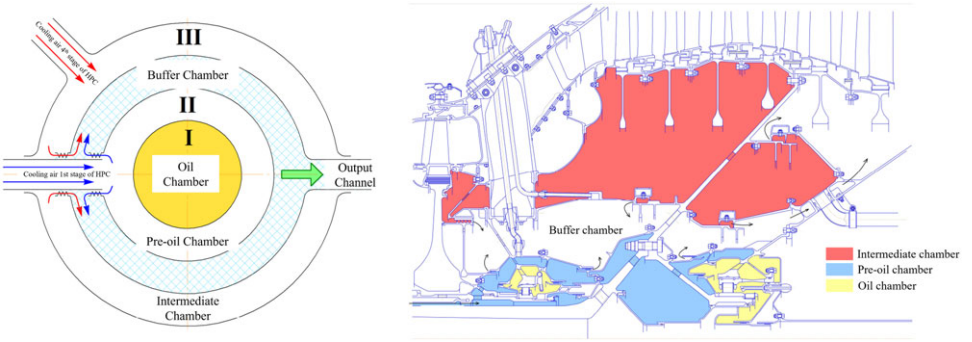


***Figure 1.*** *Diagram of the researched secondary air system cooling scheme.*

The following are the primary research points identified throughout this study:

- The impact of air seal configuration on secondary air internal system parameters (value of air bleedings on pressurisation, cooling, balancing piston and so on)
- The influence of thermal deformations on the operating radial clearance of a seal
- Heat generation in an oil chamber as a result of air seal arrangement

The temperature of the air entering the bearing chamber shall not exceed the maximum allowable temperature to prevent oil fires in the bearing chamber region. Thermal protection of the bearing chamber can be performed by minimising the surface area in contact with hot air, cooling it with air, or employing other heat flux-reducing components. The temperature of the inner surface of the wall, creating the oil chamber, is restricted. Because of the properties of the contemporary totally synthetic oils utilised, the inlet temperature of the oil chamber should not exceed 250°C, regardless of the placement of the bearing. In practice, it is difficult to satisfy this constraint. To maintain the requisite temperature in the oil chamber, unique schemes to cool the sealing system and pressurise the various seals that comprise the support seal system should be implemented.

## 2.0 Support seal system design

As part of the secondary air system, the support seal system plays a vital role in modern turbofan engines, as it flows outside the flow path used to cool vanes, blades, shrouds and disk cavities, and provides seal buffering to oil sumps. The distinctive feature of the method proposed in this work is the design of the support seal system, taking into account the mutual influence ofbuffer air seal and oil seal characteristics on the parameters of the engine oil feed systems. The development of computational fluid dynamics, which enabled study not only of a single seal but of the complete support seal system of the bearing, allowed the examination of the existing parameter connections.

The most significant of the characteristics of the support seal system to be taken into account in the design are leakage and thermo-fluid characteristics. Leakage characteristics directly influence aero engine performance (thrust and specific fuel consumption) and are determined by the geometric parametres of the labyrinth seal. Thermo-fluid characteristics also significantly influence the support seal system design on the one hand, and on the other hand are quite sensitive to the change of the seal geometric parameters (radius location and radial clearance).

The main difficulty in the joint consideration of leakage and thermo-fluid characteristics of the support seal system is that in the early stages of design, the support scheme of the aero engine, which is a determining factor for the radius location of the support seal system structure, is unknown. In addition, the calculation of the leakage without knowledge of the thermal deformations of the rotor/stator can

https://doi.org/10.1017/aer.2023.31 Published online by Cambridge University Press

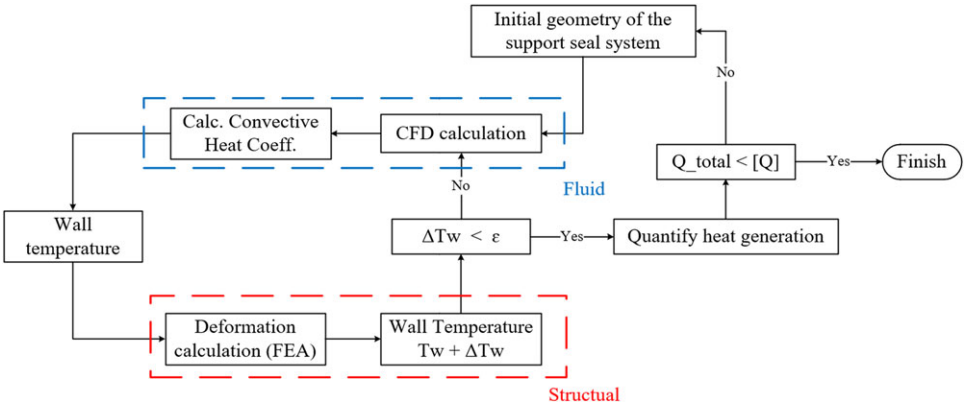


***Figure 2.*** *Design method for support seals that takes into consideration the specifications of the aero engine's oil system.*

only give approximate results. Therefore, traditionally, the formation of the geometry of the labyrinth seal occurs with a certain priority requirement of leakage, and the requirements of thermo-fluid characteristics (heat generation entering the oil chamber) are taken into account indirectly, either qualitatively or quantitatively, but on the basis of statistics and simplified mathematical models.

This is also reflected in the established order of preliminary design. The initial stage is the cold clearance design, during which the initial geometry of the sealing system is selected, and then follows the stage of synthesis of the structural-heat scheme (SHS) within a given radius location.

Taking into account the previous remarks, designing a support seal system that takes into consideration the features of an oil system is a sophisticated procedure that necessitates the creation of a particular approach, as illustrated in Fig. 2. The CFD-FEA loop is a conventional loosely coupled conjugate heat transfer/fluid-structure analysis, which comprises a numerical computational fluid model for estimating temperature distribution and convective heat transfer coefficients in all internal chambers of the system and a finite-element support seal system model. The devised approach begins with calculating the total quantity of heat entering the system from all sources and selecting the support seal system design. If the overall quantity of heat exceeds the permitted value, the system should be redesigned.

This approach is justified since, in the great majority of situations, the compressor or turbine support is sealed by multiple seals that comprise the system. The employment of a single seal for this purpose is frequently ineffective. A single seal cannot provide the required disk cooling and cavity purging, turbine shroud cooling and purging or buffering to air/oil interfaces at the bearing chambers. In other words, the seal is designed at a higher degree of design decomposition using this methodology.

The running clearances of all the seals in the system are determined based on the structural calculations and experimental investigation, and the total amount of heat entering the oil chamber and the quantity of oil pumping necessary are completed. If the needed value is not met, the seal design should be modified. The design of a support seal system is an iterative process. It enables the selection of geometric parameters for each seal and their tolerance, while taking into account oil pumping through the support of an aero engine based on a calculation of the total quantity of heat, the heat quantity from each of the sources and an analysis of their percentage ratio, which justifies the use of air cooling of support seals.

As previously stated, the growing characteristics of modern aero engines need the usage of multiple support seals rather than a single seal to provide pressurisation or cooling. As a result, this section discusses the challenges that occur in the design of support seals as part of these systems. The sealing efficiency of a seal not only impacts the amount of heat entering the bearing, but it also influences the performance of the other seals in the system in issue. As illustrated in Fig. 3, the researched support

https://doi.org/10.1017/aer.2023.31 Published online by Cambridge University Press

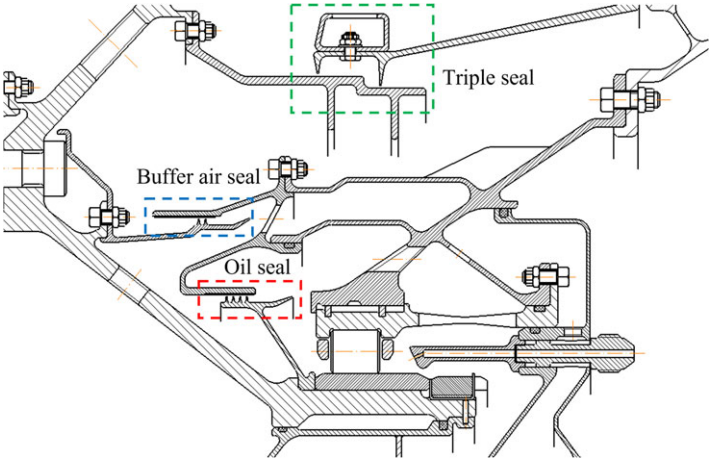


***Figure 3.*** *The investigated support seal system scheme.*

seal system contains three labyrinth seals (oil seal, buffer air seal, and triple seal), which divide the fluid domain between the rotor and stator into four chambers (oil chamber, pre-oil chamber, buffer chamber and intermediate chamber). As indicated in Table 1, labyrinth seals have an initial cold clearance.

## 3.0 Numerical methodology

A 15-degree sector CFD model was proposed to account for 3D flow characteristics in the support seal system. Because the Rinlet-1 has 24 holes and the Rinlet-2 has 32 holes, the decision was regarded as the greatest viable alternative for modeling the true, discrete geometrical characteristics of the cavity at a reasonable cost. The other structures in the cavity are virtually or completely axisymmetric. The inlet flows were considered to have assigned total pressures and uniform total temperatures.

Therefore, a study of the effect of buffer air seal location on oil seal outlet temperature was carried out in three cases. Three support seals arrangements of buffer air seal were chosen for comparison: the bottom one based on minimum cooling air flow rate and minimum heating by providing minimum knife gap area and rotor circumferential speed ($D = 314$mm), the middle one ($D = 334$mm) and the top one ($D = 354$mm). The all meshes of the CFD model were about 9M cells. The dimensionless y+ achieved is between 30 and 100, which is within the range suggested for using the conventional wall function. Figure 4 depicts the whole unstructured mesh utilised for the investigated object. Table 2 contains the boundary conditions for the numerical analysis.

As the working fluid, an ideal gas's viscosity was computed as a function of temperature using the Sutherland formula, and the heat capacity was determined using a polynomial. The turbulence model adopted was by SST, which produced findings that were most similar to experimental observations. The impact of the following parameters on the needed tightness of the studied labyrinth seal was investigated: radius of the seal location R; value of the sealing radial clearance s. A labyrinth seal, in general, can have many more geometrical parametres to regulate the leakage rate. Knife pitch, knife height, knife front and rear inclined angle and other parameters can be included. These criteria are not fundamentally important within the context of the work, hence their effect was not investigated.

The main goal of the CFD simulations is to measure the heat transfer coefficient on the support seal system's wall. The heat flux and, thus, the heat transfer coefficient should vary along the wall when flow characteristics like temperature and velocity change. The heat transfer coefficient is determined by ANSYS CFX as

$$h = Q/\left(T_w - T_{ref}\right) \tag{1}$$

https://doi.org/10.1017/aer.2023.31 Published online by Cambridge University Press

***Table 1.*** *Cold clearance of the support seal system*

| Labyrinth Seal | Clearance (mm) |
|---|---|
| Triple seal (first knife edge) | 0.8 |
| Triple seal (second knife edge) | 0.6 |
| Buffer air seal | 0.5 |
| Oil seal | 0.4 |

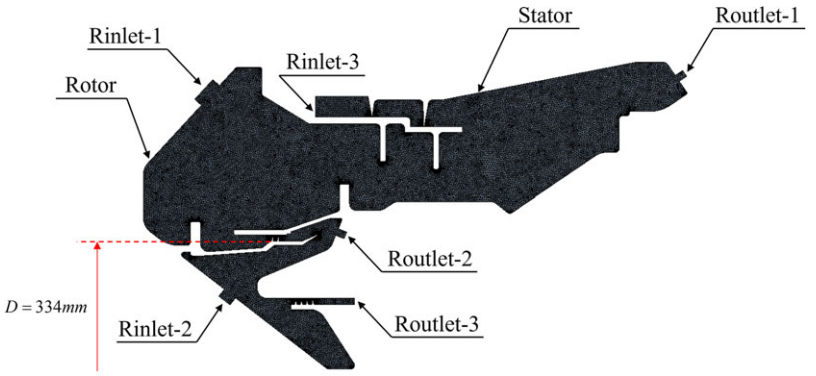


***Figure 4.*** *Unstructured mesh of the CFD model for the support seal system.*

where $T_w$ denotes the static temperature of the cell closest to the wall and $T_{ref}$ is the reference static temperature, which is set to be the second element from the wall. In this case, this formulation is not very useful, as the near wall temperature differs over the wall. The reference temperature is also used as an input in the modeling on system level, and it is more convenient to have a constant reference temperature. Because of this, the mass flow averaged temperature at the Rinlet-2 has been used as reference temperature, to determine the heat transfer coefficient rather than the near-wall temperature. This is achieved by manually specify $T_{ref}$ in the simulation set up using an expert parameter. Then, the heat transfer coefficient (HTC) is exported as a matrix comprising the coordinates and HTC for each cell along the wall, to be used in conjunction with the data for the internal cooling system. The heat transfer coefficient is radially averaged and weighted by element length to simplify the 3D heat transfer problem. The post-process calculated result of the heat transfer coefficient will be used in the following deformation analysis.

The support seal system assembly consists of rotor and stator, which are interconnected through cylindrical roller bearing, for smooth transfer of radial force. The main low-pressure shafts also act as the stiffness element to the engine rotor support system. Therefore, a 2D axisymmetric finite element model was generated in the ANSYS MECHANICAL software program to calculate the consequent deformations, as illustrated in Fig. 5. For the boundary condition, the low-pressure shaft of the rotor part was constrained by the ball bearing at the radial and axial direction, and the cylindrical roller bearing at the radial direction. The entire support seal system model is assumed axisymmetric and element type used is Plane-55. The deformation analysis is carried out in two phases. For the first phase, steady state thermal analysis has been carried out by using heat transfer coefficient (shown in Fig. 6) and bulk temperatures as boundary conditions. The inputs from this analysis are used for getting thermal deformations. For the second phase, the support seal system was analysed under normal speeds (N1 = 2,800rpm), with corresponding thermal expansion, which was calculated from the steady state thermal analysis.

The necessity to analyse the combined work of the entire support seal system complicated the investigation. Because of changes in the radial clearance in the seals produced by thermal expansion of the structural sections, a temperature change in one chamber induces a temperature change in all chambers.

https://doi.org/10.1017/aer.2023.31 Published online by Cambridge University Press

***Table 2.*** *Boundary conditions*

| Boundary Condition | Parameter |
|---|---|
| Rinlet-1 | $p_1^* = 257119$pa, $T_1^* = 476$K |
| Rinlet-2 | $p_1^* = 157097$pa, $T_1^* = 371$K |
| Rinlet-3 | $p_1^* = 334255$pa, $T_1^* = 400$K |
| Routlet-1 | p = 251553pa |
| Routlet-2 | p = 151553pa |
| Routlet-3 | p = 112770pa |

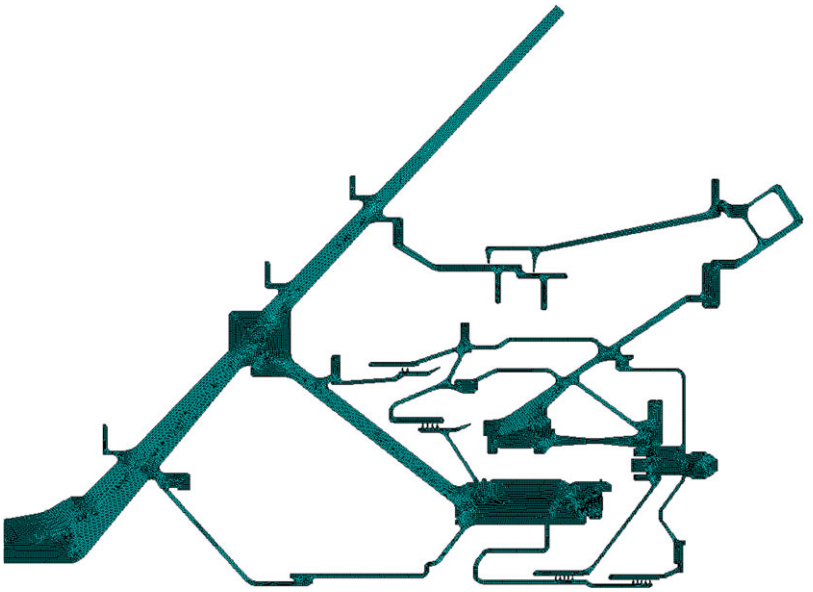

***Figure 5.*** *Finite element model for structural analysis of the support seal system.*

As a result, the calculation should be run several times to determine the operating radial clearance value for each design alternative, which is illustrated in Fig. 2. At each iteration, the boundary conditions, including the heat transfer coefficient and the displacement of the seal model, were updated. According to the investigated support seal system, it has reached wall temperature convergence after four iterations as usual. Figure 7 shows the effect of the buffer air seal's radius of position on the temperature distribution in the support seal system.

Figure 7(a) depicts the conventional design. Figure 7(b) depicts the temperature distribution when the radius is lowered by 10mm, whereas Fig. 7(c) depicts the temperature distribution when the radius is raised by 10mm. The radius changes, causing the area of the sealing gap to fluctuate as well. As a result, a 10mm radius decrease reduces the temperature in the pre-oil cavity by 5°C. By increasing the radius, the gas temperature in the pre-oil cavity rises by up to 13°C, causing heating conduction of the oil seal and an increase in the operating seal radial clearance in this seal. It is evident that having as small a radius as feasible is preferable to reducing the magnitude of heat flow into the bearing with leaking working fluid. However, in this scenario, it is vital to consider, first and foremost, the change in clearance between the rotor and stator caused by temperature spreading and centrifugal forces.

It is clear from the temperature field analysis that having as small a buffer air seal radius as feasible is preferable to reducing the magnitude of heat flow into the bearing with leaking working fluid; but, it still needs to consider the pressure distribution difference between a higher radius and a lower radius, as

https://doi.org/10.1017/aer.2023.31 Published online by Cambridge University Press

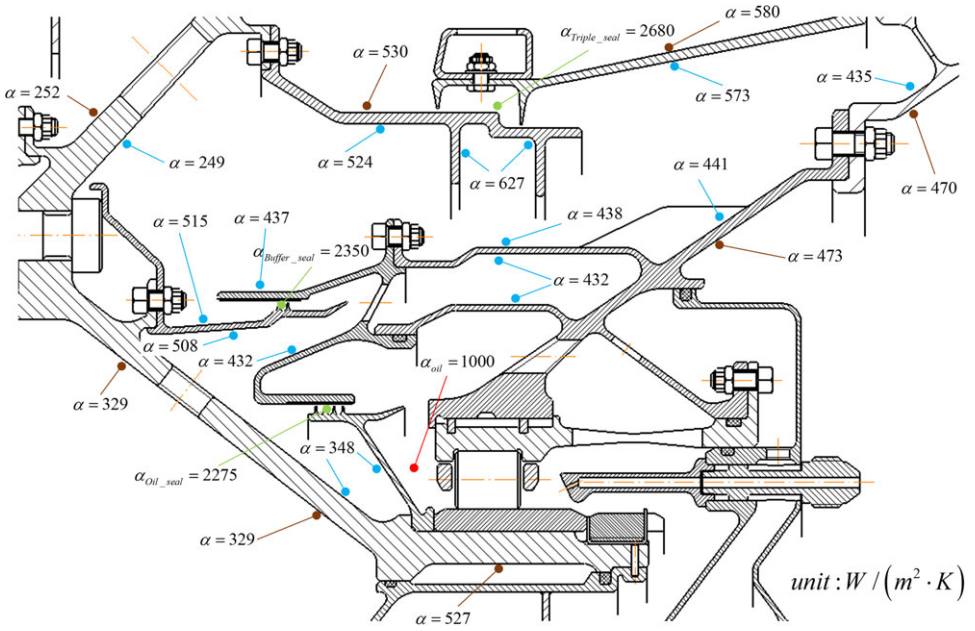


***Figure 6.*** *Convective heat transfer coefficient distribution over turbine support seal system surfaces.*

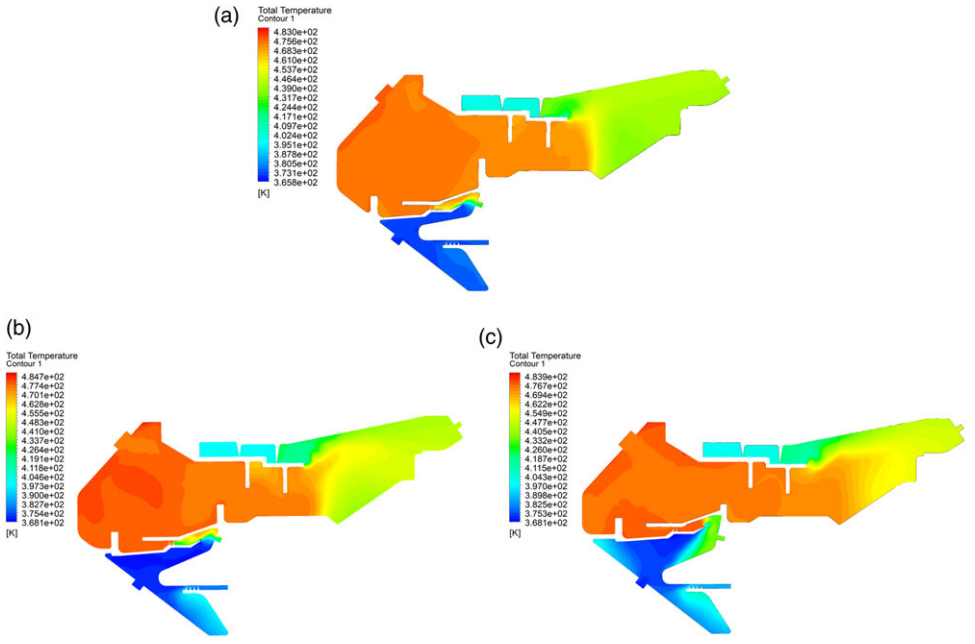


***Figure 7.*** *Change of temperature distribution depending on the radius of the buffer air seal position: (a)* $\Delta R = -10mm$*; (b)* $\Delta R = 0mm$*; (c)* $\Delta R = 10mm$*.*

https://doi.org/10.1017/aer.2023.31 Published online by Cambridge University Press

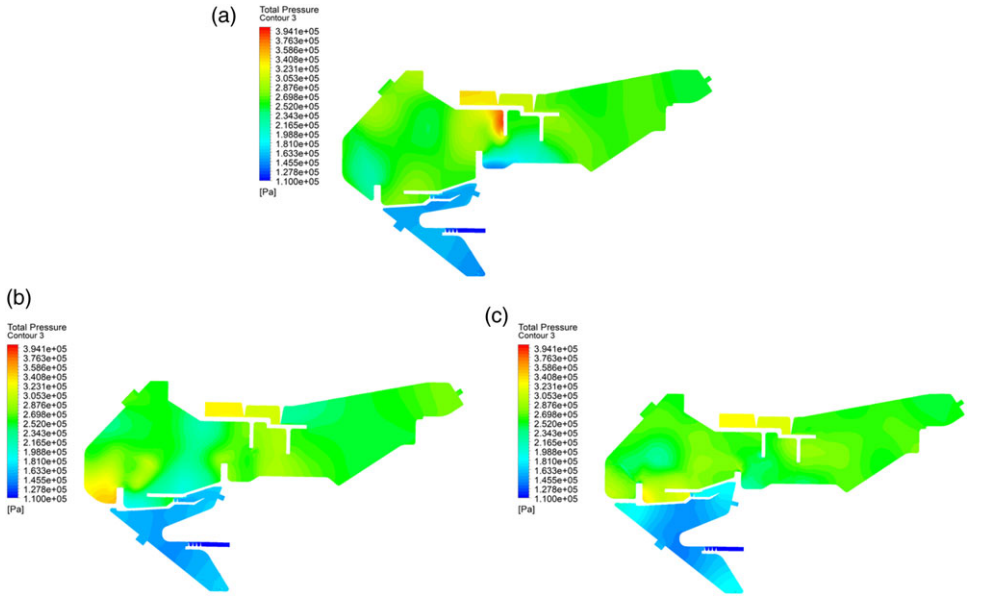


***Figure 8.*** *Change of pressure distribution depending on the radius of the buffer air seal position: (a)* $\Delta R = -10mm$*; (b)* $\Delta R = 0mm$*; (c)* $\Delta R = 10mm$*.*

shown in Fig. 8, to help understand how to choose a reasonable buffer air seal radius that is preferable for reducing leakage into the bearing. For the given radius location of the buffer air seal, due to the reduction in flow area and a smaller pressure difference, a lower radius leads to less leakage of the buffer air seal. In this work, it is important to investigate the interaction between the buffer air seal and the oil seal. As shown in Fig. 8, with the reduction of buffer air seal radius, the pressure difference between the oil seal increase from 1.26 to 1.45. For the leakage analysis of the oil seal, it could be concluded that a smaller radius of buffer air seal causes less thermal deformation of the oil seal but increases the pressure difference. Therefore, in this scenario, it is vital to consider conducting the experimental tests, to verify the preliminary analytical results of the CFD-FEA method and investigate the change in clearance between the rotor and stator of the oil seal caused by temperature spreading and centrifugal forces.

Figure 9 depicts the integrated deformation results of the support seal system with thermal expansion and centrifugal effect. Figure 10 depicts the change in clearance caused by the above mentioned loads in the oil seal (a), buffer air seal (b), andt seal (c). The figure shows that the change in clearance caused by stator deformations is substantially greater than that caused by rotor deformations, which is explained by the stator's greater thermal inertia. It is 1.25 times greater for the oil seal, 2.2 times higher for the buffer air seal, and 1.8 times higher for the triple seal. Despite the fact that rotor and stator parts deform in the same direction, the application of temperature and centrifugal loads causes a decrease in the nominal value of the operating radial clearance. In this situation, the oil seal gap was lowered by 0.06mm, the buffer air seal gap was reduced by 0.08mm and the triple seal gap was reduced by 0.15mm. This indicates that a further reduction in radial clearance of the oil seal, together with a matching drop in operating clearance, might result in rotor-stator contact.

## 4.0 Experimental test

### *4.1 Test facility*

The experiments were carried out using the Institute of Advanced Aero Engine Design's sealing test equipment (AAED). The test rig was established based on the research of stability of aero engine low

https://doi.org/10.1017/aer.2023.31 Published online by Cambridge University Press

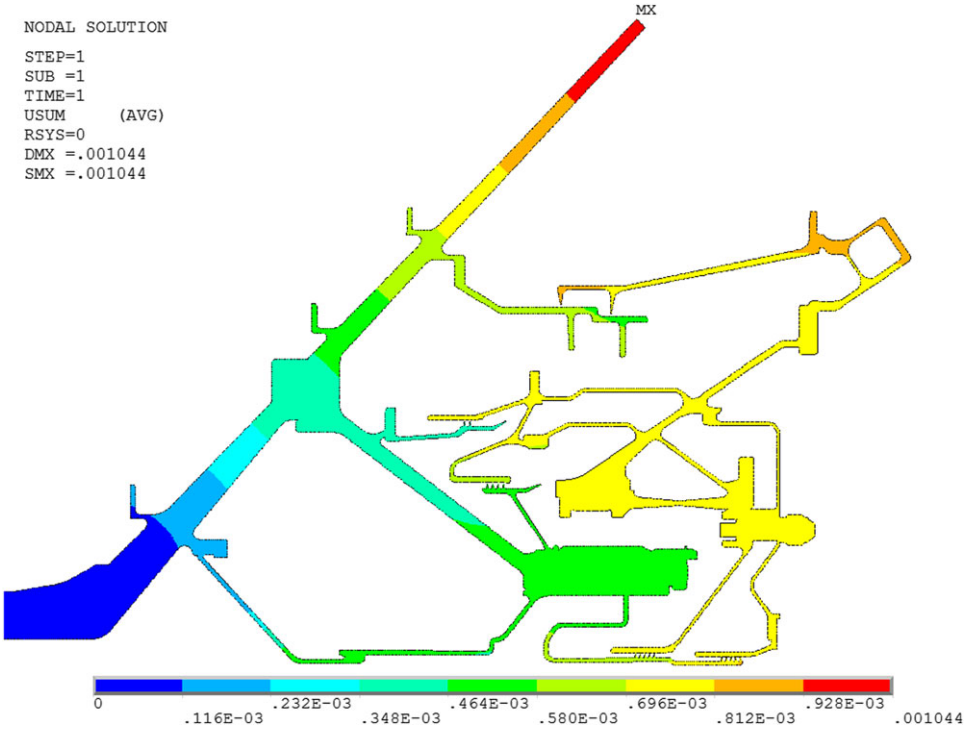


***Figure 9.*** *Deformation of turbine support seal system.*

pressure turbine secondary air system, which includes several labyrinth seals and internal chambers. The test rig could be used to study the performance of the support seal system, which includes the buffer chamber, the pre-oil chamber, and the oil chamber. It has a rotor that could be swapped out for different radius of labyrinth seals. An air supply system, an air heater, an air mixing section, a test measurement section, an inlet and outlet temperature and pressure control system, and a sensor measurement system comprise the designed test rig. The turbine flow metre is used to measure the airflow out of the pre-oil chamber, which is equivalent to the flow entering the oil chamber through the oil seal. Power was supplied by a 10kW electric motor with a maximum speed of 20,000rpm. The rotational speed was measured using a torque sensor installed on the rear of the motor. The air supply system is pressurised with both positive and negative relative pressures through two control valves that could be adjusted to a few Pascals accuracy. The pressure at each point of the internal chamber is measured transiently by the miniature dynamic pressure sensor, and the temperature is measured by the thermocouple with a response rate of 0.01s.

### *4.2 Test condition*

In general, engine state parameters such as pressure, temperature and rotational speed are high, and direct experimental simulation is expensive. Based on the similarity principle, the pressure, temperature and rotational speed of the experiment should be suitably reduced based on the experimental state being similar to each physical field of the engine condition. Furthermore, the geometrical structural characteristics of the engine model and the experimental model are kept same during the analytical procedure. The state parametres of the experimental test in this example, analysed by the approximate modelling principle, are mass flow discharge coefficient and windage heating coefficient. These two dimensionless parameters are equal in the experimental and engine models, making it easier to apply the results of

https://doi.org/10.1017/aer.2023.31 Published online by Cambridge University Press

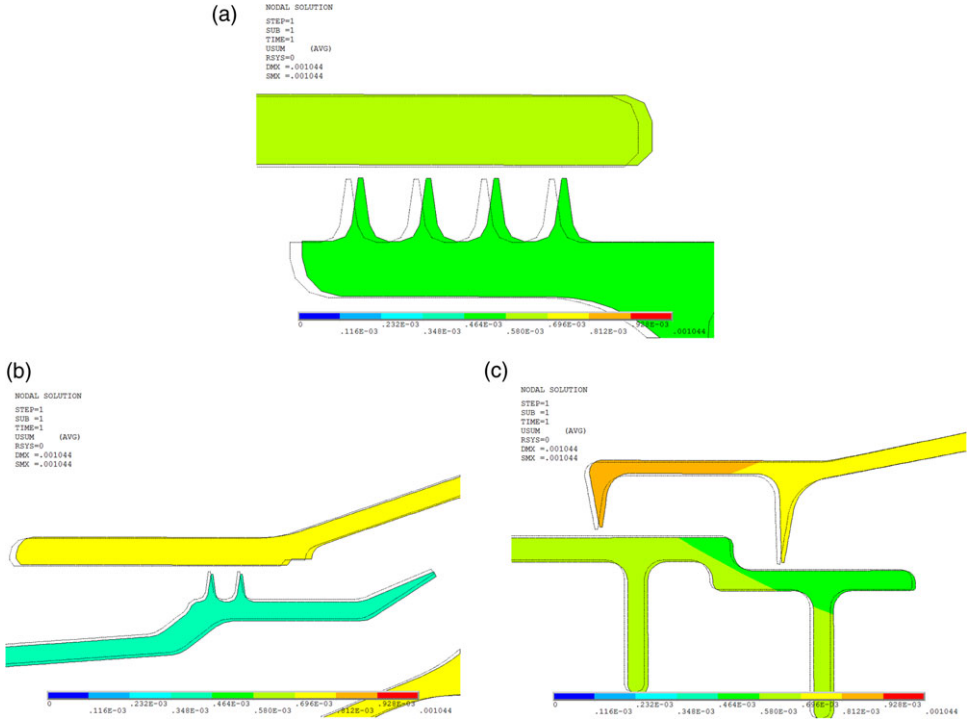


***Figure 10.*** *Change of running clearance in the (a) oil seal, (b) buffer air seal, and (c) triple seal from thermal expansion and centrifugal load.*

this work to the engine states. Therefore, according to the working conditions of an aero engine and experiments, the test conditions were investigated, as given in Table 3.

A thermal growth impact is predicted when the stator temperature changes with the increasing radius position of the top buffering seal in Fig. 11. During the experimental test, it was difficult to cause the change of stator deformation by the temperature of R-inlet2 airflow. Therefore, changes in geometric parameters of the stator due to excessive local heat generation in the engine oil feed system was simulated by an electromagnetic rapid heating ring. Heating temperature is obtained from CFD calculations, as shown in Fig. 7. The oil seal radial clearance was dynamically measured during the test using a fiber optic displacement sensor for the dynamic test.

Therefore, the test is divided into two types: those with a heating ring and those without. As a result of these tests, the oil seal outlet temperature and running clearance were determined. The value of oil seal power loss will be compared between experiment and the CFD-FEA method using the experiment-by-hand calculation shown in Section 5, which helps to validate the effectiveness of the method proposed in Section 2.

## 5.0 Quantify heat generation

There are large heat fluxes in the support seal system during operation. It is critical to identify and measure heat production since it has a significant impact on engine performance. It raises the working temperatures of the components, reducing their durability. Calculating heat generation necessitates the use of geometry data for the components, material properties and heat transfer coefficients (HTC). These parameters are difficult to determine, thus empirical factors are frequently employed to assess them.

https://doi.org/10.1017/aer.2023.31 Published online by Cambridge University Press

***Table 3.*** *Test conditions*

| Condition | Parameter | Value |
|---|---|---|
| Aero engine | Rotational speed | 2,800rpm |
| | Inlet temperature | 371K |
| | Inlet pressure | 157,097pa |
| | Outlet pressure | 11,2770pa |
| | Rotational speed | 2,507rpm |
| Experiments | Inlet temperature | 300K |
| | Inlet pressure | 11,2830pa |
| | Outlet pressure | 80,994pa |

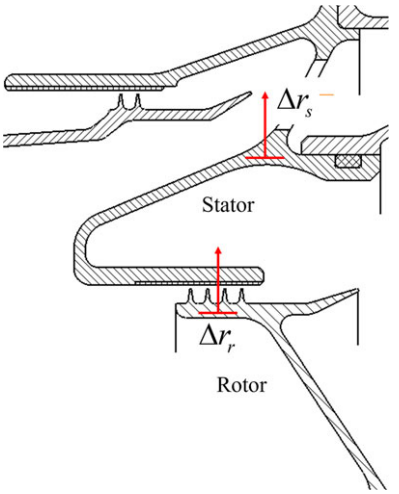


***Figure 11.*** *Thermal expansion of the stator/rotor.*

As shown in Fig. 12, the most important heat fluxes in the support seal system are located in the flow channel, support walls, shaft, leakage through the seals, and friction in the bearings, gearings and splines. The total quantity of heat entering the support seal system is then calculated using the following formula:

$$Q_{\Sigma} = Q_{wall} + Q_{leakage} + Q_{shaft} + Q_{bearing} + Q_{gearings,splines} \tag{2}$$

In the following section, we will look at a theoretical calculation for calculating the quantity of heat generated by various sources in the investigated support seal system.

### *5.1 Heat conduction through the walls*

It is vital to note that the heat transfer coefficient (HTC) may only be computed using a design value. The HTC values along the seal and the support walls in the investigated support seal system are difficult to determine through the experimental test; thus, the calculated results from CFD-FEA analysis were employed to assess them. The heat flux conducted from the wall to the oil chamber is then calculated using Newton-Richman's law.

$$Q_{wall} = \sum_{i=1}^{n} [\alpha_i F_i (T_{wall} - T_{oil})] \tag{3}$$

https://doi.org/10.1017/aer.2023.31 Published online by Cambridge University Press

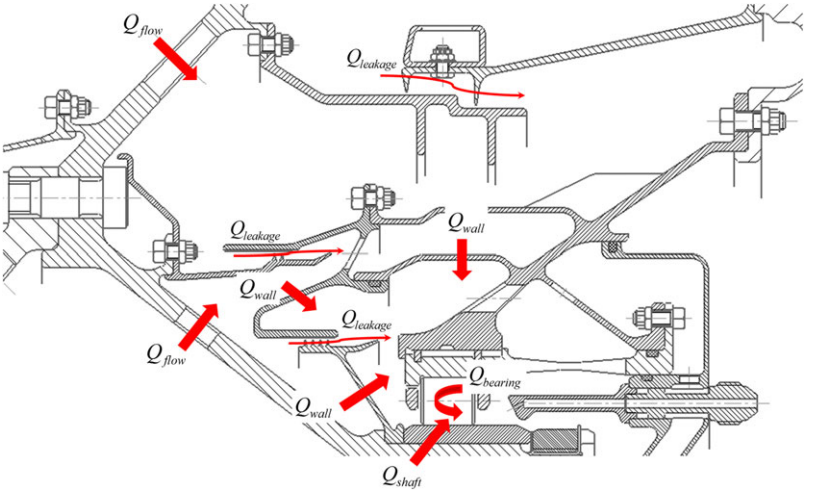


***Figure 12.*** *Source of heat generation in the support seal system.*

Where $\alpha_i$ denotes the heat transfer coefficient, $F_i$ denotes area of the outer surface of the wall, $T_{wall}$ denotes the temperature of the outer side of the wall, $T_{oil}$ denotes the temperature of the oil near the wall of the bearing in the oil chamber.

The heat flux entering the outer wall from the air can be represented as:

$$Q_{wall} = \alpha \left[ \left( F_s - F_p \right) + \eta_P F_P \right] \left( \bar{T}_{in} - \bar{T}_{wall} \right) \tag{4}$$

$$Q_{wall} = \alpha_{cyl} F_s \left( \bar{T}_{in} - \bar{T}_{wall} \right) \tag{5}$$

$$\alpha_{cyl} = \alpha \left[ \left( \eta_p - 1 \right) \frac{F_p}{F_s} + 1 \right] \tag{6}$$

Where $\alpha$ denotes the heat transfer coefficient of the air, $F_s$ denotes the surface area of the smooth wall, $F_p$ denotes the surface area of the fin, $\bar{T}_{in}$ denotes the average temperature of air at the inlet to the support seal system, $\bar{T}_{wall}$ denotes the average wall temperature over the cylindrical surface.

The fin efficiency coefficient ($\eta_p$) with respect to the fin area ($F_p$) is determined by the following equation:

$$\eta_p = \sqrt{\frac{\lambda_{wall} \Pi_p}{\alpha F_p}} th \left( \sqrt{\frac{\alpha \Pi_p}{\lambda_{cm} F_p}} h_p \right) \tag{7}$$

Where $\lambda_{wall}$ denotes wall thermal conductivity, $\Pi_p$ denotes the fin circumference, $F_p$ denotes the surface area of fin, $h_p$ denotes the height of fin.

The overall heat transfer coefficient through the cylindrical wall of the support seal system will be calculated as follows:

$$K = \frac{1}{\frac{1}{\alpha_{air}} + \frac{\delta_{wall}}{\lambda_{wall}} + \frac{1}{\alpha_{oil}}} \tag{8}$$

Where $\delta_{wall}$ denotes the wall thickness. To determine the value of the overall heat transfer coefficient, in addition to the geometric parameters, it is necessary to know the heat transfer coefficients $\alpha_{air}$ and $\alpha_{oil}$, which are found from the known criterial equations.

As shown in Fig. 13, there are three major walls to consider in the researched support seal system. Therefore, the amount of heat transferred through both sides of the wall is determined by the following formula:

https://doi.org/10.1017/aer.2023.31 Published online by Cambridge University Press

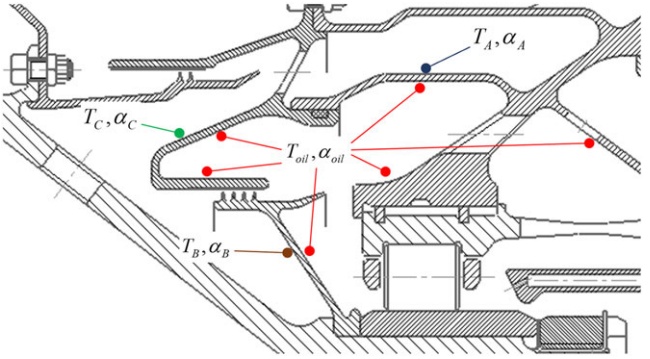


***Figure 13.*** *Heat generation through the walls in the support seal system.*

$$Q_{wall} = \sum_{i=1}^{n} K_{\Sigma} F_i \left(\bar{T}_{air,i} - \bar{T}_{oil,i}\right) \tag{9}$$

Where, $\bar{T}_{air}$ denotes the average temperature of the air near the outer walls, $\bar{T}_{oil}$ denotes the temperature of the oil near the inner walls, which can be determined by the following relationship, taking into account the heating of oil in the friction units of the sealing system:

$$\bar{T}_{oil} = T_{in,oil} + \Delta T_{friction} \tag{10}$$

For conical walls represented as a set of cylindrical walls, the average heat transfer coefficient is determined as follows:

$$K_{\Sigma} = \sum_{i=1}^{n} \frac{1}{\frac{1}{\alpha_{air,i}} + \frac{\delta_{wall,i}}{\lambda_{wall,i}} + \frac{1}{\alpha_{oil}}} \tag{11}$$

Finally, the following dependency was developed to calculate heat generation through the walls:

$$K_{\Sigma} = \sum_{i=1}^{n} Q_{wall} = \sum_{i=1}^{n} \frac{F_i \left(\bar{T}_{air,i} - \bar{T}_{oil}\right)}{\frac{1}{\alpha_{air,i}} + \frac{\delta_{wall,i}}{\lambda_{wall,i}} + \frac{1}{\alpha_{oil}}} \tag{12}$$

### *5.2 Heat conduction through the leakage*

The second component (the amount of heat produced with leakage through the seal) in Equation (2) is calculated by the formula:

$$Q_{leakage} = \sum_{i=1}^{n} \dot{m}_i C_p (T_{out} - T_{in}) \tag{13}$$

Where $\dot{m}_i$ denotes air mass flow rate through seals, $C_p$ denotes specific heat capacity of air, $T_{in}$ denotes the air temperature at inlet of the seal, $T_{out}$ denotes the air temperature at outlet of the seal. Heat transfer and rotational work transfer (windage heating) cause the change in total air temperature.

### *5.3 Heat conduction through the cylindrical roller bearing*

Most rolling bearings operate at relatively low speeds and loads. The heat dissipation from the bearing through the housing and shaft and its lubrication in an oil chamber is sufficient to ensure the satisfactory thermal condition of such bearings. The greatest amount of heat enters the bearing through the oil, and much of the heat could be transferred through the housing and shaft during engine startup and shutdown.

https://doi.org/10.1017/aer.2023.31 Published online by Cambridge University Press

V.M. Demidovich et al. [12] devised a technique for detecting heat emission in aviation engine rolling bearings in the second part of the 1970s. The author identified friction losses and losses from oil mixing as causes of heat release using similarity criteria. The following dependency was developed to estimate the heat dissipation (W) of friction in these bearings:

$$Q_{bearing} = C\beta z\rho l^2 u^3 \tag{14}$$

Where $C$ denotes total drag coefficient, $\beta$ denotes coefficient taking into account the effect of radial clearance on power loss, $z$ denotes number of rolling elements in the bearing, $\rho = 1180.37 - 0.753T$ denotes oil density, $l$ denotes the diameter of the rolling elements, $u$ denotes circumferential speed of the bearing cage.

The total drag coefficient can be found by the formula:

$$C = 1.26\mathrm{Re}^{-0.5}Eu^{-0.5} + 46.5 \times 10^3\mathrm{Re}^{-1}\mathrm{Pr}^{-0.8} \tag{15}$$

The Reynolds criterion is found from the ratio:

$$\mathrm{Re} = \frac{ul}{v} \tag{16}$$

Where $v = 0.0276 \times 2.71828^{((3609.58(\frac{1}{T} - \frac{1}{311.11}) + 776568(\frac{1}{T} - \frac{1}{311.11})^2))}$ denotes the kinematic viscosity of the oil.

Prandtl criterion is equal to:

$$\mathrm{Pr} = \frac{C_p v\rho}{k} \tag{17}$$

Where $k = 0.148676 - 0.000222153\ (T - 366)$ denotes thermal conductivity of the oil.

The Euler criterion can be found by the formulas:

$$Eu = \frac{10F_m}{\rho(ul)^2} \tag{18}$$

$$F_m = \frac{2.92F_r + zF_c}{2z} \tag{19}$$

$$F_c = 1225\frac{l^3u^2}{d_m} \tag{20}$$

Where $F_m$ denotes the average load on the bearing, $F_r$ denotes the radial load on the bearing, $F_c$ denotes the centrifugal load of the rolling elements in the bearing.

The circumferential speed of the bearing cage can be found using the formula:

$$u = \frac{\pi(d_m - l)\,n}{120} \tag{21}$$

Where $d_m = \frac{D+d}{2}$ denotes the diameter of the centre of gravity of the bearing, equal to the half-sum of the inner and outer diameters.

The coefficient $\beta$ in Equation (14) is found by the formula:

$$\beta = 1 + 1.7\left(0.1 - h_{bearing}\right) \tag{22}$$

Where $h_{bearing}$ denotes the value of radial clearance in the bearing.

### *5.4 Heat conduction through the shaft*

The third component of Equation (2) is analogous to the conduction of heat through walls. The following formula could be used to determine it:

$$Q_{shaft} = \alpha A(T_{air} - T_{oil}) \tag{23}$$

https://doi.org/10.1017/aer.2023.31 Published online by Cambridge University Press

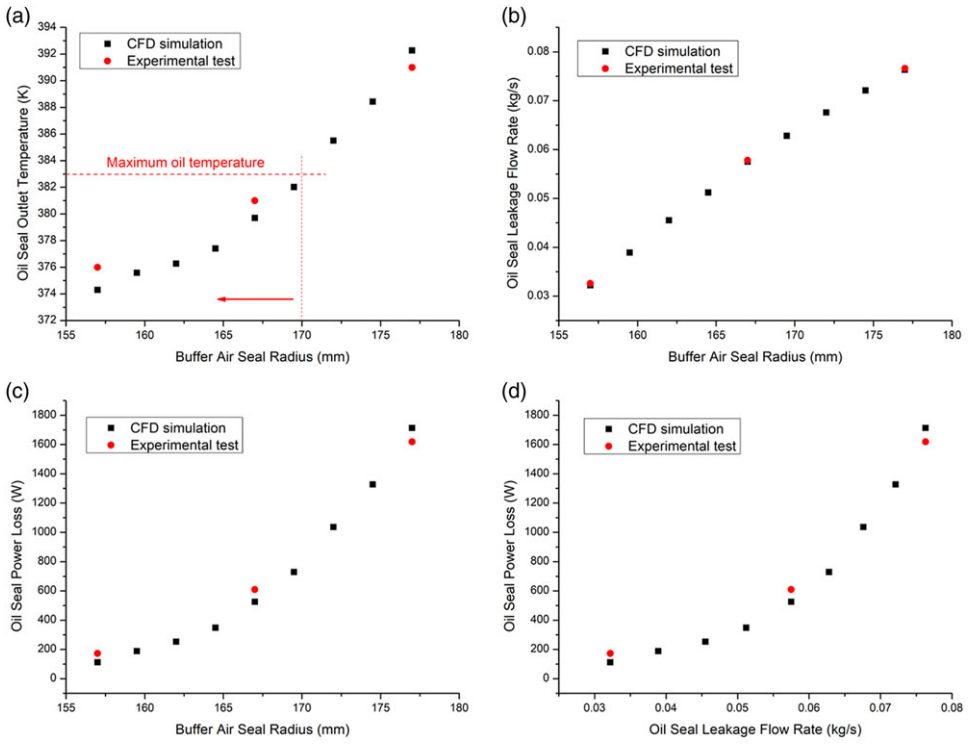


***Figure 14.*** *Investigate the radius of the buffer air seal position on the (a) oil seal outlet temperature, (b) oil seal leakage flow rate, (c) oil seal power loss and (d) oil seal power loss.*

### *5.5 Heat conduction through the gears, splines*

In general, each bearing has a number of gears and splines. Because of the geometry and kinematics of teeth, friction in gear systems differs in certain ways. It comprises rolling and sliding actions. To calculate the heat generated by friction in gear and spline systems, use the following equation:

$$Q_{gearings,splines} = (1 - \eta)\, N \tag{24}$$

Where $\eta$ denotes the efficiency of gearing system, $N$ denotes the transmitted power (W). For more accurate calculations, the special literature recommends using the experimental dependence obtained by A.I. Petrusevich [13]:

$$Q_{gearings,splines} = N \frac{\pi \varepsilon_s f}{K \cos \beta_g} \left( \frac{1}{Z_K} \pm \frac{1}{Z_k} \right) \tag{25}$$

Where $\varepsilon_s$ denotes the contact ratio, $f$ denotes coefficient of friction, $\beta_g$ denotes the angle of inclination of teeth to the axis of rotation of the starting cylinder (for helical and chevron gears), $Z_K$ and $Z_k$ denote the number of teeth. The ratio $f/K$ varies from 0.015 to 0.045.

## 6.0 Results and discussion

First, the results of the test without the heating ring are examined. Results of the investigation into the radius position of the buffer air seal separating the pre-oil and buffer chambers are shown in Fig. 14. When the radius increases, the air flow to the oil and to the pre-oil chamber will also increase. An increase in flow rate will lead to an increase in temperature. Both the temperature in the pre-oil chamber and the oil chamber will increase simultaneously. However, the temperature increase in the oil chamber

https://doi.org/10.1017/aer.2023.31 Published online by Cambridge University Press

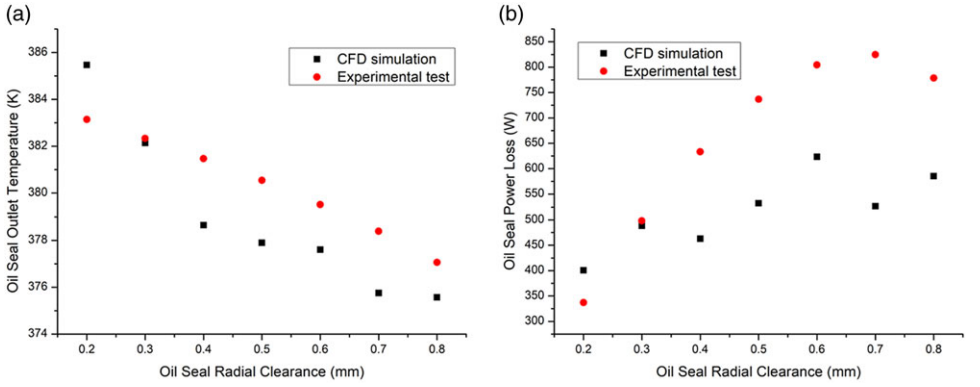


***Figure 15.*** *Investigate the radial clearance of the oil seal on the (a) oil seal outlet temperature, (b) oil seal power loss.*

is severely limited. This is due to both the properties of the oil and the operation of the rolling bearings. In this case, a temperature value of 383K was taken as the limit value (horizontal line in Fig. 14(a)). This constraint, in turn, leads to a restriction on the maximum radius value. It is limited to a rise of no more than 1.8% of the nominal value. As shown in Figs. 14(b), (c), and (d), there is good agreement on the buffer air seal radius, oil seal leakage flow rate, and oil seal power loss between the experimental results and the CFD-FEA analysis. However, in this case, the effect shown in Fig. 11 has not been found and it is necessary to perform the next test with a heating ring.

For the test with the heating ring, it was conducted into the oil seal and investigated the variations in the quantity of heat entering into the oil chamber with air from varied clearance values. As demonstrated in Fig. 15, as the oil seal radial clearance rises, the oil seal outlet temperature decreases, the oil seal power loss has a significant divergence between the experimental test and CFD-FEA loosely coupled method. The temperature rise variation of the loosely coupled method in predicting the variable clearance process and the experimental results differ by up to 3.2°C. According to the seal power loss calculation Equation (12), the leakage flow rate increases as the clearance increases, while the outlet temperature rise decreases as the clearance increases; thus, the relative magnitude of the ratio of leakage flow rate change to temperature rise change determines the trend of seal power loss as the oil seal running clearance changes. Because the loose coupling method does not take into account the combined effect of structural thermal deformation on seal leakage flow rate and outlet temperature rise, the predicted power loss results differ from the experimentally measured results. The power loss of the seal is proportional to the values of leakage flow rate and temperature rise, and the leakage flow and temperature rise exhibit an inverse trend with clearance change. The experimental test results show that the power loss of the oil seal is greatest when the gap is 0.7mm, that the influence of leakage flow rate on the power loss of the seal is particularly strong in the interval less than 0.7mm, that the change in temperature rise is smaller in the interval greater than 0.7mm, and that the change ratio of the leakage flow rate is less than the change ratio caused by temperature rise, resulting in a slight decrease of the oil seal power. Thus, to avoid out-of-range power loss, a reasonable range of radial clearance could be chosen based on the above analysis.

Finally, according to the experimental test temperature and clearance, combined with the heat generation calculation methods in Section 5, Table 4 summarises the heat generation calculation results for the support seal system. The friction in the bearings transfers the majority of the heat to the oil chamber. The total of the heat transmitted through the bearing chamber walls and the power loss from leakage through the seal is greater than 30%. This scenario proves the tightness of each seal in the cooling support seal system significantly influences the lubrication oil consumption. Therefore, to get the lubrication oil consumption required for adequate cooling, it necessitates detailed estimates of support seal system

https://doi.org/10.1017/aer.2023.31 Published online by Cambridge University Press

***Table 4.*** *Variables for heat generation calculation*

| Heat Sources | Symbol | Amount of Heat (W) |
|---|---|---|
| Support walls | $^{Q}wall$ | 2,637 |
| Shaft | $^{Q}shaft$ | 261 |
| Leakage | $^{Q}leakage$ | 633 |
| Bearings | $^{Q}bearing$ | 5,795 |
| Gearings and splines | $^{Q}gearing,splines$ | 353 |
| Total | $Q_{\Sigma}$ | 9,679 |

heat generation. Bich et al. [14] devised the following calculation, which could be used to calculate the estimated rate at which lubrication oil needs to be pumped into the oil chamber.

$$W = 6 \times 10^{4} \frac{Q_{\Sigma}}{C_{p,mix}\rho_{mix}\Delta T_{mix}} \tag{26}$$

Where, $Q_{\Sigma}$ denotes the total heat transferred to the bearing chamber with different sources, $C_{p,mix}$ denotes the specific heat capacity of the oil-air mixture under mean temperature of the bearing chamber, $\rho_{mix}$ denotes the density of the oil-air mixture, $\Delta T_{mix}$ denotes temperature difference between the inlet and outlet of the bearing chamber.

The total heat transferred to the bearing chamber from all sources is 9,679W. With the amount of heat transmission to the support seal system known, we can now calculate the required rate of pumping oil through the aero engine support from Equation (26) to be around 8.43L/min.

## 7.0 Conclusion

The quantitative interrelation of the turbine support cooling scheme with the value of oil pumping through the support was established using the developed CFD-FEA loosely coupled method of support seals design, taking into account the parameters of the oil feed system. The research conducted allows for the selection of the radius location of the buffer air seal and the radial clearance of the oil seal while taking into account the parameters of the oil feed system and increasing the overall efficiency of the engine.

Based on current mathematical models for estimating heat generation from individual sources situated in the support seal system, a methodology for assessing the heat balance inside the aero engine turbine support is developed, allowing the effect of each of the heat sources to be estimated. It is demonstrated that the distribution ratio and value of heat generation entering the bearing chamber, which is directly dependent on seal tightness and seal radius location and is carried in through the bearing chamber walls and with flow leakage, reach 30%. The heat production quantifies the analytical approach in the support seal system, which will allow you to identify the reasonable aspects of an individual seal design and devise strategies to enhance them. In the system under examination, a 10% change in the radius of the labyrinth seal resulted in a 4.5% increase in radial deformation of the oil seal stator and a 32.5% increase in leakage through the oil seal. When the seal system is considered as a whole, it is feasible to sensibly pick the characteristics of each seal, reducing the overall time for engine tuning.

The implementation of the experimental approach demonstrated the importance of collaborative design in the support seal system. The experimental test was performed to validate the preliminary CFD-FEA loosely coupled analysis result, which revealed that in a turbine support seal system, the leakage flow rate of the oil seal was primarily influenced by the structural deformation of the oil seal's rotor and stator parts, which was influenced by the radius of the buffer air seal. Heat conduction through leakage to the bearing chamber is connected with the leakage flow rate and the outlet temperature rise of the oil seal, which should be examined in the experimental testing. Comparing with the CFD-FEA loosely

https://doi.org/10.1017/aer.2023.31 Published online by Cambridge University Press

coupled method, the experimental results showed that the seal power loss needs to consider the pressure difference and the structural deformation caused by the thermal and centrifugal effects together.

**Acknowledgements.** This work was supported by funding from the Aero Engine Advanced Technology International Cooperation Project (2020-I-0629-0060). Authors acknowledge the support of China Scholarship Council, Institute of Advanced Aero Engine Design (AAED), Faculty of Aerospace Engineering, Northwestern Polytechnical University.

## References

[1] Ludwig, L. and Johnson, R. Sealing technology for aircraft gas turbine engines, *10th Propulsion Conference*, October 1974, **74**, pp 256–282.
[2] Povinelli, V.P. Current seal designs and future requirements for turbine engine seals and bearings, *J. Aircraf*, 1975, **12**, pp 266–273.
[3] Proctor, M.P. and Delgado, I.R. Leakage and power loss test results for competing turbine engine seals, *Turbo Expo 2004*, 2004, **4**, pp 441–451.
[4] Chupp, R.E., Hendricks, R.C., Lattime, S.B. and Steinetz, B.M. Sealing in turbomachinery, *J. Propuls. Power*, May 2006, **22**, (2), pp 313–349.
[5] Chew, J.W. and Hills, N.J. Computational fluid dynamics for turbomachinery internal air systems, *Philos. Trans. Royal Soc. A*, May 2007, **365**, (1859), pp 2587–2611.
[6] Aslan-zada, F.E., Mammadov, V.A. and Dohnal, F. Brush Seals and Labyrinth Seals in gas turbine applications, *Proc. Inst. Mech. Eng. A: J. Power Energy*, November 2012, **227**, (2), pp 216–230.
[7] von Plehwe, F.C., Krug, M.B., Höfler, C. and Bauer, H.J. Experimental and numerical investigations on oil leakage across labyrinth seals in aero engine bearing chambers, *ASME Turbo Expo 2016*, June 2016, **1**, pp 441–451.
[8] Flouros, M., Cottier, F., Hirschmann, M. and Salpingidou, C. Numerical investigation on windback seals used in aero engines, *Aerospace*, November 2018, **5**, (1), pp 12–27.
[9] Li, G., Zhang, Q., Lei, Z., Huang, E., Wu, H. and Xu, G. Leakage performance of labyrinth seal for oil sealing of aero-engine, *Propuls. Power Res.*, March 2019, **8**, (1), pp 13–22.
[10] Li, G., Zhang, Q., Lei, Z., Huang, E., Wu, H. and Xu, G. Leakage performance of floating ring seal in cold/hot state for aero-engine, *Chinese J. Aeronaut.*, March 2019, **32**, (9), pp 2085–2094.
[11] Ilieva, G. and Pirovsky, C. Labyrinth seals with application to turbomachinery, *Proc. Inst. Mech. Eng. A: J. Power Energy*, May 2019, **50**, (5), pp 479–491.
[12] Petrov, N.I., and Lavrentyev, Yu.L. Comparison of heat generation estimation methods for angular contact ball bearings, *VESTNIK SSAU*, July 2018, **17**, (2), pp 154–163.
[13] Petrov, N.I. *Principal Conclusions from Contact-Hydrodynamic Theory of Lubrication*, Associated Technical Services Publishers, 1951.
[14] Bich, M.M., Weynberg, E.V. and Surnov, D.N. *Lubrication of Aircraft Gas Turbine Engines*, Mashinostroenie Press, Moscow, 1979.

**Cite this article:** Sun P. and Liu C. (2023). Quantifying the impact of heat in support seal configuration for aero engines. *The Aeronautical Journal*, **127**, 1698–1716. https://doi.org/10.1017/aer.2023.31